Immunity
Article

A *Shigella* Effector Dampens Inflammation by Regulating Epithelial Release of Danger Signal ATP through Production of the Lipid Mediator PtdIns5P

Andrea Puhar,[1,2,*] Hélène Tronchère,[3,4] Bernard Payrastre,[3,4,5] Guy Tran Van Nhieu,[6,7,8,9] and Philippe J. Sansonetti[1,2,9,*]
[1]Inserm U786
[2]Institut Pasteur
Unité de Pathogénie Microbienne Moléculaire, 75724 Paris Cedex 15, France
[3]Inserm U1048
[4]Université Toulouse 3
I2MC, 31432 Toulouse Cedex 4, France
[5]CHU Toulouse, Laboratoire d'Hématologie, 31432 Toulouse Cedex 4, France
[6]Inserm U1050
[7]CNRS UMR7241
[8]Collège de France
Equipe Communication Intercellulaire et Infections Microbiennes, CIRB, 75231 Paris Cedex 5, France
[9]These authors are co-senior authors
*Correspondence: andrea.puhar@pasteur.fr (A.P.), philippe.sansonetti@pasteur.fr (P.J.S.)
http://dx.doi.org/10.1016/j.immuni.2013.11.013

SUMMARY

Upon infection with *Shigella flexneri*, epithelial cells release ATP through connexin hemichannels. However, the pathophysiological consequence and the regulation of this process are unclear. Here we showed that in intestinal epithelial cell ATP release was an early alert response to infection with enteric pathogens that eventually promoted inflammation of the gut. *Shigella* evolved to escape this inflammatory reaction by its type III secretion effector IpgD, which blocked hemichannels via the production of the lipid PtdIns5P. Infection with an *ipgD* mutant resulted in rapid hemichannel-dependent accumulation of extracellular ATP in vitro and in vivo, which preceded the onset of inflammation. At later stages of infection, *ipgD*-deficient *Shigella* caused strong intestinal inflammation owing to extracellular ATP. We therefore describe a new paradigm of host-pathogen interaction based on endogenous danger signaling and identify extracellular ATP as key regulator of mucosal inflammation during infection. Our data provide new angles of attack for the development of anti-inflammatory molecules.

INTRODUCTION

Initiation of inflammation in the absence of infection (e.g., sterile tissue damage and autoimmune diseases) depends on the detection of endogenous danger signals. These molecules are constitutively present inside host cells (i.e., they are "self") but, after release, their extracellular presence signals danger to the immune system (Bours et al., 2006). In contrast, it is thought that initiation of inflammation during infection depends on the detection of microbial patterns ("non-self"), which translates into production of and response to classical proinflammatory mediators such as cytokines, chemokines, and lipidic mediators (Kawai and Akira, 2011).

Extracellular ATP (eATP) has gained recognition as endogenous signaling molecule in immunity and inflammation (Bours et al., 2006). Its extracellular concentration is negligible in healthy tissues, because extracellular enzymes quickly degrade it. After release, ATP modulates inflammation in a concentration-dependent manner upon binding to purinergic receptors. Both purinergic receptors and ectoenzymes are ubiquitously expressed. In immune and nonimmune cells, eATP induces cell type-specific responses ranging from NF-κB activation, expression of adhesion molecules and proinflammatory mediators, enhanced phagocytosis and migration (Bours et al., 2006), to activation of the NLRP3 inflammasome (Mariathasan et al., 2006). Nevertheless, a major role for eATP in infectious diseases has not been recognized so far.

Shigella is a Gram-negative pathogen causing bacillary dysentery. The primary symptom of infection is mild to bloody-mucoid diarrhea owing to inflammatory destruction of the colonic mucosa (Phalipon and Sansonetti, 2007). *Shigella* is endowed with a type III secretion system, which injects an array of effector molecules into host cells to force bacterial entry and dissemination, and to manipulate the immune response (Parsot, 2009; Phalipon and Sansonetti, 2007). The effector IpgD is injected during invasion (Niebuhr et al., 2000) and acts as PtdIns(4,5)P_2 4-phosphatase, yielding the poorly studied lipid PtdIns5P (Niebuhr et al., 2002). In vitro IpgD shows various effects on host cells such as alteration of plasma membrane tension (Niebuhr et al., 2002) and activation of the kinase Akt (Pendaries et al., 2006; Ramel et al., 2011) in HeLa cells, and inhibition of T lymphocyte migration (Konradt et al., 2011). However, its role during disease remains unclear.

During *Shigella* invasion, epithelial cells release ATP through hemichannels composed of connexin (Cx) 26 or 43 (Tran Van

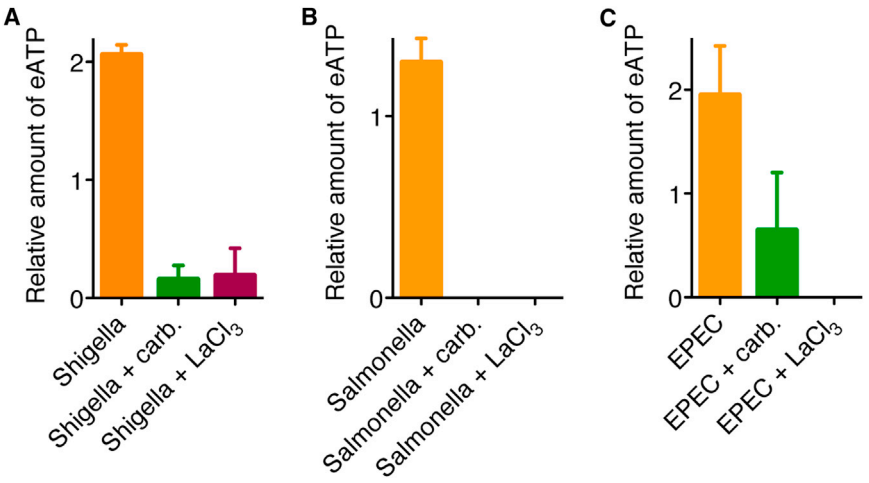

Figure 1. Infection of Polarized Intestinal Epithelial Cells with Bacterial Pathogens Induces Hemichannel-Dependent ATP Release

Polarized TC7 cells were infected with WT (A) *Shigella* at MOI 1:40 for 10 min, (B) *Salmonella* at MOI 1:2.5 for 3 min, or (C) EPEC at MOI 1:2.5 along with BSA-treated activated charcoal to adsorb eATP for 2 hr. ATP was quantified in the supernatant or after elution from charcoal with a firefly luciferase-luciferin assay. Concentrations were in the nM range. Values were normalized to those of noninfected samples, which were set to 1 and subtracted. The mean with SD of one representative experiment of three performed in triplicates or quadruplicates is shown. Carb., carbenoxolone, 60 μM; $LaCl_3$, 20 μM. See also Figure S1.

Nhieu et al., 2003), stimulating bacterial capture by filopodia (Romero et al., 2011). Importantly, the pathophysiological consequence of ATP release on the outcome of *Shigella* infection and its regulation are not understood. Further, it is not known whether infection of epithelial cells with pathogens other than *Shigella* also induces regulated ATP release.

Here we describe an innate immune response against infection with enteric pathogens, which is initiated by infected epithelial cells through hemichannel-dependent release of ATP and mediates early immune recognition and induction of inflammation. We showed that *Shigella* blocked ATP release through IpgD-mediated production of PtdIns5P. Thus, we identify regulated ATP release as a key process during infection-induced mucosal inflammation, providing new targets for the development of anti-inflammatory therapy.

RESULTS

Intestinal Epithelial Cells Infected with *Shigella*, *Salmonella*, or EPEC Release ATP

To determine whether regulated ATP release is a common response to infection, we challenged epithelial cells with pathogens other than *Shigella*. Infection of polarized intestinal epithelial (TC7) cells, which express Cx26, Cx32, and Cx43 (Clair et al., 2008), with *Salmonella enterica* serovar Typhimurium or with enteropathogenic *Escherichia coli* (EPEC) led to appearance of eATP, similarly to *Shigella* (Figure 1). Concentrations of eATP were normalized to allow the comparison of independent experiments. Hemichannel inhibitors carbenoxolone or $LaCl_3$ dampened ATP release, in accordance with previous findings that ATP is released through hemichannels during infection of HeLa-Cx-transfectants with *Shigella* (Tran Van Nhieu et al., 2003). Hemichannel inhibitors did not compromise bacterial viability (see Figures S1A–S1I available online) nor did the pathogens alter viability of infected cells (Figures S1J–S1L). The eATP content of bacterial suspensions was negligible (data not shown). These experiments indicate that hemichannel-dependent ATP release is a common epithelial response to infection with enteric pathogens.

IpgD Inhibits ATP Release In Vitro

To identify effectors that might alter hemichannel function and thereby ATP release, we focused on *Shigella*. Infection of HeLa-Cx26-transfectants cells with *ipgD*-deficient *Shigella* resulted in eATP concentrations that increased over time and were significantly higher compared with the wild-type (WT) and the noninvasive *mxiD* mutant (Figure 2A). Complementation with a plasmid encoding *ipgD* resulted in its overexpression (Figure S2A) and inhibited the appearance of eATP (Figure 2B). Further, ATP release upon infection with the *ipgD* mutant was abolished in cells treated with hemichannel inhibitors 18α-glycyrrhetinic acid (AGA), CELAb2—a Cx26, Cx32, and Cx43-hemichannel blocking antibody (Clair et al., 2008)—carbenoxolone, or $LaCl_3$ (Figure 2C–D). Similar results were obtained with polarized TC7 cells (Figures 2E and 2F, Figures S2B and S2C). Plaque formation assays showed that WT and *ipgD*-deficient *Shigella* are equally invasive in HeLa (Allaoui et al., 1993a) and in polarized TC7 cells (Figure S2D). The intracellular ATP concentration of cells infected with *ipgD*-deficient *Shigella* decreased moderately, which excluded that elevated eATP was due to enhanced ATP production (Figure S2E).

For comparison with IpgD, cells were challenged with *sopB*-deficient *Salmonella*, because SopB was reported to hydrolyze phosphoinositides (Marcus et al., 2001; Norris et al., 1998; Zhou et al., 2001). Infection of HeLa-Cx26 cells and polarized TC7 cells with the *sopB* mutant did not result in higher eATP concentrations with respect to WT *Salmonella*, indicating that SopB does not regulate hemichannel-dependent ATP release (Figures S2F and S2G).

Together, these experiments showed that IpgD dampens the appearance of eATP through inhibition of hemichannels during *Shigella* infection in vitro.

IpgD Blocks Hemichannels through Production of PtdIns5P

To gain insight into the inhibitory mechanism of IpgD and to validate our results in a system independent of eATP, we performed a dye uptake assay in transfected HeLa-Cx26 cells. Transient expression of GFP-tagged proteins did not alter the number of hemichannels on the cell surface (Figures S3A and S3B).

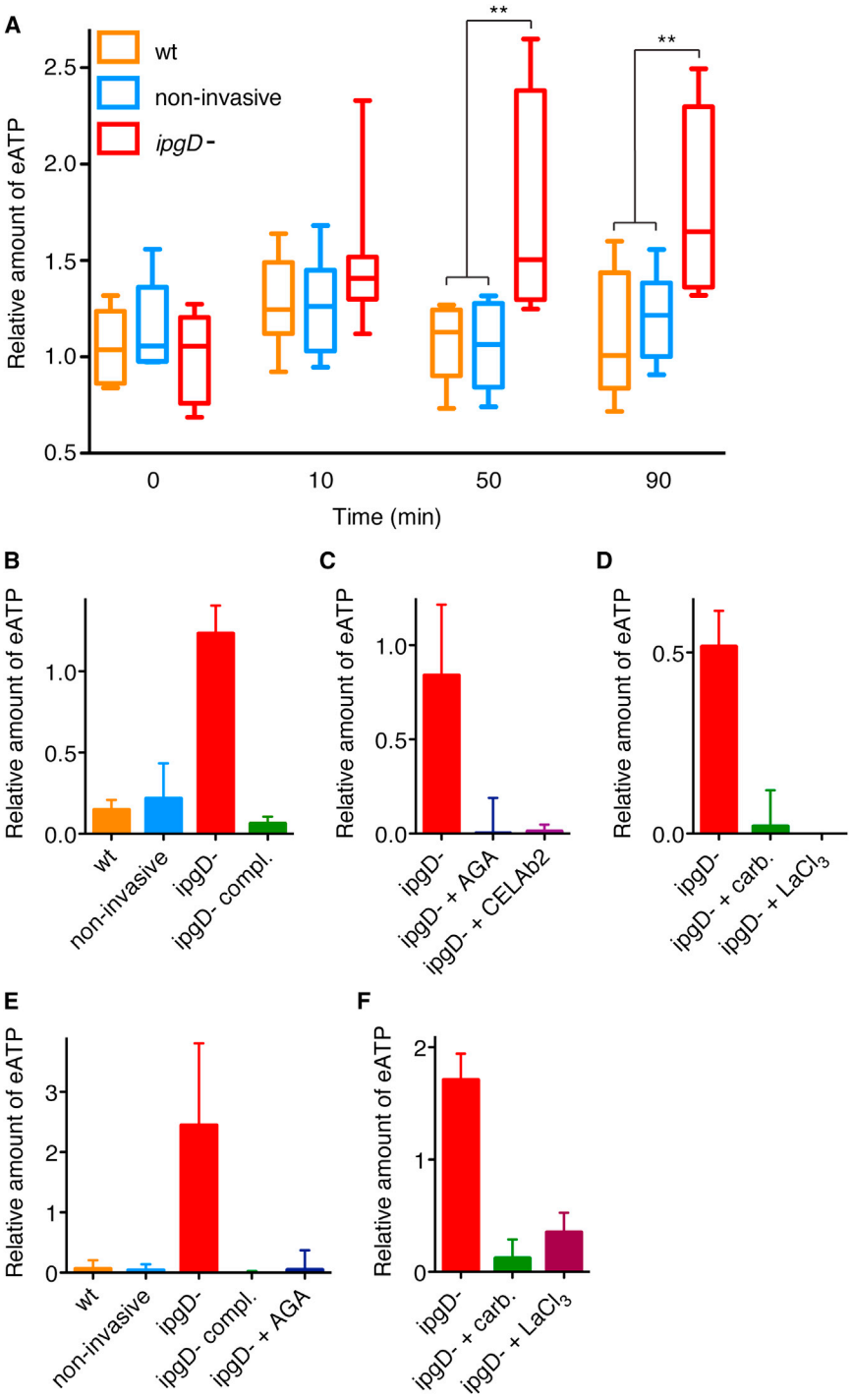

Figure 2. IpgD Inhibits Hemichannel-Dependent ATP Release in Epithelial Cells In Vitro

(A–D) HeLa-Cx26 and (E and F) polarized TC7 cells were infected with *Shigella* at MOI 1:5 and 1:40, respectively, for (C and D, F) 30 min or (B and E) 90 min. ATP was quantified in the supernatant with a firefly luciferase-luciferin assay. Concentrations were in the nM range. Values were normalized to those of noninfected samples, which were set to 1 and subtracted. (A) The median with minima and maxima of eight independent experiments performed in quadruplicates, analyzed by a one-way ANOVA followed by a Bonferroni post hoc test, is shown. $^{**}p < 0.01$. (B–F) The mean with SD of one representative experiment of three performed in quadruplicates is shown. AGA, 18α-glycyrrhetinic acid, 100 μM; CELAb2, hemichannel-blocking antibody; carb., carbenoxolone, 60 μM; $LaCl_3$, 20 μM. See also Figure S2.

Similarly to infection, transiently expressed IpgD blocked dye uptake, but expression of a phosphatase-dead IpgD mutant allowed normal hemichannel function (Figure 3A). Pretreatment with AGA or CELAb1 or CELAb2 repressed dye loading, confirming that dye passage is specific to hemichannels. Transient expression of a PtdIns(4,5)P_2 5-phosphatase (Inp54p), which converts similar amounts of PtdIns(4,5)P_2 as IpgD, but to PtdIns4P (Pendaries et al., 2006), had no effect on hemichannel opening (Figure 3B), indicating that IpgD modulates hemichannel activity by increasing PtdIns5P, rather than by reducing PtdIns(4,5)P_2 levels. Similar results were obtained with HeLa-Cx43 cells (Figures S3C and S3D). To further investigate the importance of PtdIns5P in hemichannel regulation, we preincubated TC7 cells with PtdIns5P and assayed ATP release under low Ca^{2+} conditions. The presence of exogenous PtdInsPs did not compromise cellular viability (Figure S3E). Unlike PtdIns3P and PtdIns4P, PtdIns5P inhibited ATP release at concentrations superior or equal to 1 pM—corresponding to 1,000 molecules per cell (Figure 3C). Moreover, in polarized TC7 cells PtdIns5P "complemented" *ipgD*-deficient *Shigella* in an ATP release assay (Figure 3D). These experiments showed that PtdIns5P, either exogenous or produced by IpgD, prevents hemichannel opening.

IpgD Inhibits ATP Release In Vivo

We then wished to confirm our findings in vivo and to assess the pathophysiological consequence of ATP release during *Shigella* infection. Importantly, no noninvasive methods to measure eATP in vivo are described. The task is complicated by the fact that eATP is unstable and rapidly degraded to adenosine, inosine, and uric acid (Bours et al., 2006). Hence, we infected ligated ileal loops in rabbit—a well-established model to evaluate the phenotype of *Shigella* strains—in the presence of BSA-treated activated charcoal to adsorb and thereby protect eATP in the intestinal lumen. Activated charcoal did not compromise viability of intestinal epithelial cells and bacteria or invasiveness of *Shigella*

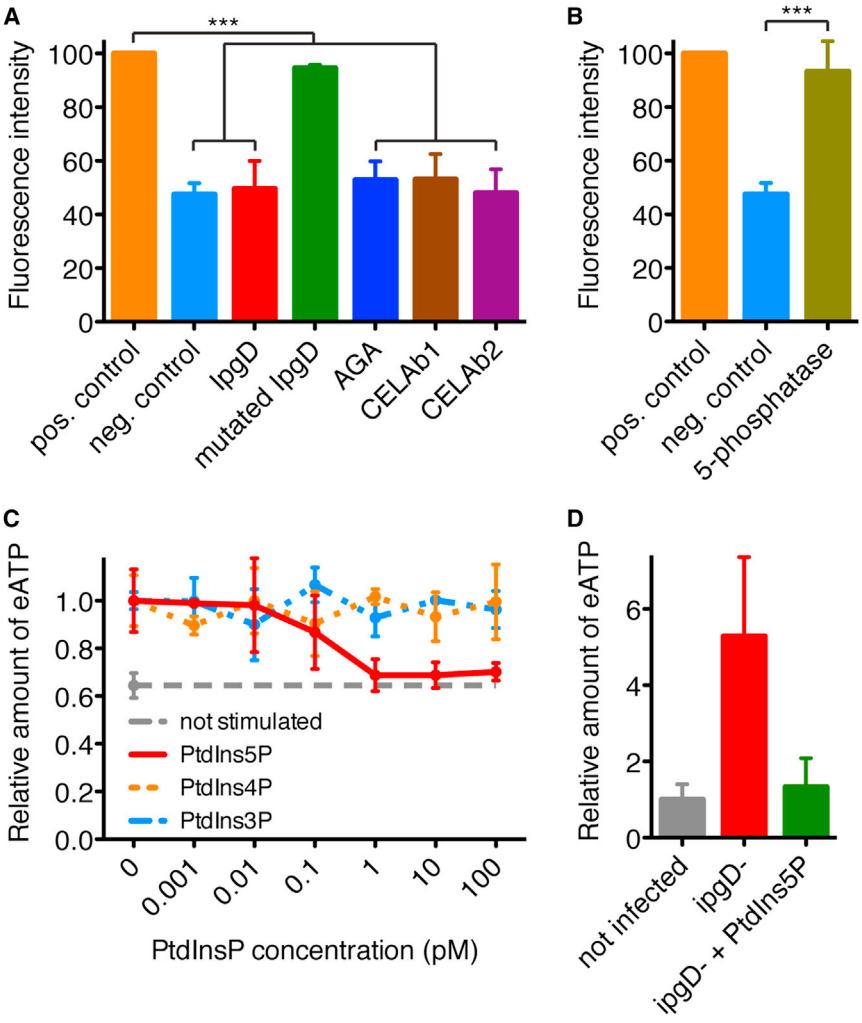

Figure 3. PtdIns5P Controls Hemichannel Opening

(A and B) GFP-tagged proteins of interest (GFP only for controls) were transiently expressed in HeLa-Cx26 cells, and hemichannel opening was induced by exposure to low Ca^{2+} buffer (except for negative controls). Uptake of the hemichannel-permeable, plasma membrane-impermeable dye ethidium bromide was quantified by fluorescence in transfected cells. Values were normalized to those of positive controls, which were set to 100. The mean with SD of 2349 and 1478 cells in (A) and (B), respectively, from three independent experiments, analyzed by a one-way ANOVA followed by a Bonferroni post hoc test, are shown. ***$p < 0{,}001$. AGA, 18α-glycyrrhetinic acid, 100 μM; CELAb1/2, hemichannel-blocking antibodies.

(C) TC7 cells were treated with 10-fold dilutions of PtdIns5P, PtdIns4P, or PtdIns3P, and hemichannel opening was induced by exposure to low Ca^{2+} buffer. ATP was quantified in supernatants with a firefly luciferase-luciferin assay. Concentrations were in the nM range. Values were normalized to those of positive controls. Means with SD of triplicates of one representative experiment of three are shown.

(D) Polarized TC7 cells were infected with *ipgD*-deficient *Shigella* for 50 min in the presence or absence of 1 nM PtdIns5P. ATP was quantified in supernatants with a firefly luciferase-luciferin assay. Values were normalized to those of noninfected samples. The mean with SD of quadruplicates from one representative experiment of three is shown. See also Figure S3.

(Figure S4). Elevated eATP was found at early stages (4 hr) of infection with the *ipgD* mutant compared to WT, noninvasive, and *ipgD*-complemented strains (Figure 4A), in keeping with diminished ATP release owing to IpgD-mediated hemichannel closure. Accordingly, carbenoxolone and $LaCl_3$ suppressed ATP release (Figure 4B). In a separate set of experiments, we quantified ATP degradation products in the intestinal lumen after 4 hr of infection (omitting coinjection of charcoal). As for eATP, levels of ATP degradation products peaked in the absence of IpgD (Figure 4C). Carbenoxolone and $LaCl_3$ inhibited the accumulation of ATP degradation products (Figure 4D), indicating that they originated from eATP released across hemichannels. Adenosine, inosine, and uric acid concentrations in rabbit blood were negligible (data not shown). Together, these experiments showed that IpgD inhibits the appearance of eATP through inhibition of hemichannels in vivo.

ATP Release Precedes Intestinal Inflammation

Real-time PCR analysis of intestinal tissues from rabbits infected for 4 hr showed that expression of selected proinflammatory cytokines and antimicrobial peptides did not change or was occasionally very slightly upregulated for *ipgD*-deficient *Shigella* in the absence of charcoal only (Tables S1–S4), indicating that ATP release precedes a shift in cytokine profile. Histological sections showed that the epithelium was intact (Figure 5A; Figure S5A), confirming that ATP was not shed because of mucosal damage. However, in-depth analysis showed that upon infection with the *ipgD* mutant, in the absence of charcoal, the structure of villi was slightly altered: they were broadened due to axial edema and beginning influx of leukocytes (Figure 5B). For WT *Shigella*, only few histological changes could be observed. Similar histological results were obtained in newborn mice (Figure S5B).

IpgD Dampens eATP-Dependent Inflammation

At later stages of intestinal infection in rabbits (6–8 hr) *ipgD*-deficient *Shigella* led to a massive increase of proinflammatory cytokines and antimicrobial peptides—particularly IL-1β, IL-6, IL-8, IL-12p40, IL-17A, IL-23, IFN-γ, TNFα, LeuP, and CAP18 (Figure 6A, Table S5). The cytokine profile was oriented toward a proinflammatory Th17 cell response, as previously described for WT *Shigella* (Schnupf and Sansonetti, 2012; Sellge et al., 2010). Interestingly, eATP was reported to promote the differentiation of Th17 lymphocytes (Atarashi et al., 2008). Enhanced cytokine production correlated with an extremely severe destruction of the mucosa compared with the WT (Figure 6B). This hyperinflammatory phenotype was readily reverted by

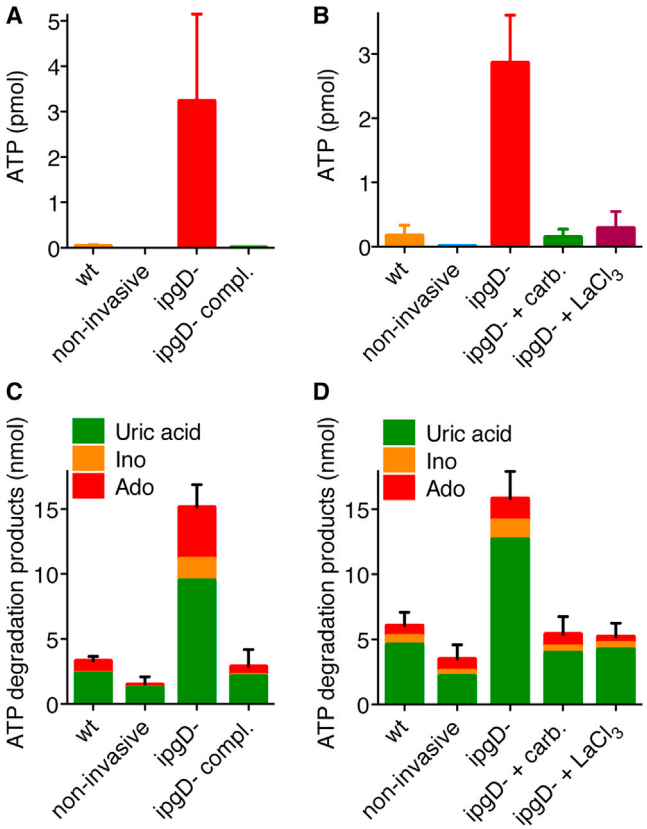

Figure 4. IpgD Inhibits Hemichannel-Dependent ATP Release at Early Stages of Infection In Vivo

Ligated ileal loops of rabbits were infected with *Shigella* for 4 hr.

(A and B) BSA-treated activated charcoal was injected along with bacteria and recovered at the end of infection, and adsorbed ATP was eluted. ATP was quantified with a firefly luciferase-luciferin assay. The mean of duplicate loops with SD from one representative animal of four per condition is shown.

(C and D) Loops were rinsed with 0.9% NaCl solution to collect luminal content. ATP degradation products adenosine, inosine, and uric acid were quantified with a fluorescence assay. The sum of the means of duplicate loops with the propagated error (SD) from one representative animal of four per condition is shown. Ado, adenosine; Ino, inosine. Carb., carbenoxolone, 20 μM; $LaCl_3$, 20 μM. See also Figure S4.

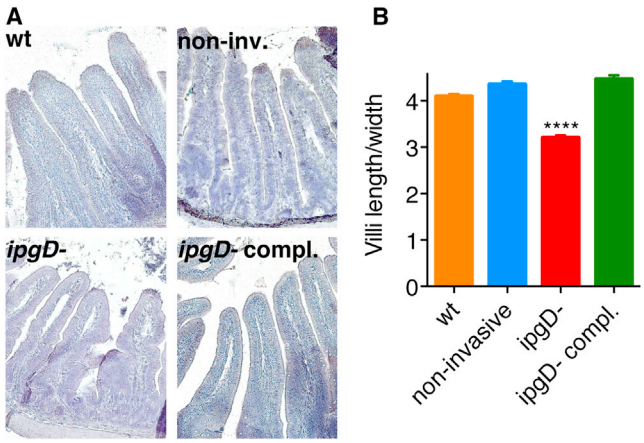

Figure 5. Early Signs of Inflammation Can Be Observed upon Infection with *ipgD*-Deficient *Shigella*

Ligated ileal loops of rabbits were infected with *Shigella* for 4 hr. Histological analysis of samples 4C-D is shown.

(A) *Shigella*-LPS was labeled immunohistochemically (red), and sections were counterstained with hematoxylin.

(B) The mean with SEM of the length to width ratio of 2,265 villi, analyzed by a one-way ANOVA followed by a Bonferroni post hoc test, is shown. ****p < 0.0001. See also Figure S5 and Tables S1–S4.

ipgD-complementation (Figure 6; Table S5). Moreover, as anticipated after 4 hr of infection, at later stages the *ipgD* mutant caused strong edema inside the lamina propria (Figure 6B), which was accompanied by accumulation of fluid in the lumen (Figure S6A). This phenotype provided additional support for IpgD-mediated inhibition of ATP release and ensuing accumulation of degradation products, because 5′-adenosine monophosphate (AMP) and adenosine induce isotonic fluid release in intestinal epithelial cells (Madara et al., 1993). Therefore, eATP-derived adenosine could cause diarrhea during shigellosis.

To strengthen the causal link between IpgD-inhibited ATP release and induction of inflammation, we attempted to reduce the aggressiveness of the *ipgD*-deficient strain by blocking eATP-dependent signaling and to expand the destructive potential of the WT by introducing eATP. Indeed, the breadth of the inflammatory response was strongly diminished in loops infected with *ipgD*-deficient *Shigella* in the presence of suramin, an inhibitor of purinergic receptors (Figures 7A and C; Table S6). Suramin did not affect bacterial viability (Figure S1E). Likewise, coinjection of apyrase, which dephosphorylates eATP, dampened mucosal damage induced by the *ipgD* mutant (Figures 7B and 7C; Table S7). Interestingly, in apyrase-treated samples, we observed a striking accumulation of fluid in the tissue and the lumen (Figure 7C; Figure S6B). In contrast, injection of nonhydrolysable ATPγS along with WT *Shigella* boosted its inflammatory phenotype, leading to an unprecedented production of proinflammatory cytokines and recruitment of leukocytes (Figures 7B and 7C; Table S7). ATPγS alone did not cause leukocyte recruitment and inflammation (data not shown; Table S7), in keeping with a previous report showing that macrophages do not migrate toward ATPγS (Isfort et al., 2011).

DISCUSSION

Our results indicate that ATP release accelerates the onset of and exacerbates inflammation, indicating that it acts as endogenous danger signal during *Shigella* infection. To establish an infection, *Shigella* needs to escape early immune recognition by injecting IpgD. To our knowledge, this is the first report of a microbial factor inhibiting the release of an endogenous danger signal, which highlights the importance of endogenous danger signaling to the immune response against infection.

We propose that in the intestinal mucosa, hemichannel-dependent ATP release is an early and swift alert response to infection. We advance the following succession of events for *Shigella*: hemichannels open when *Shigella* engages in invasion, sending out a "message of distress." The eATP concentration rises and is sensed and amplified in an autocrine and paracrine

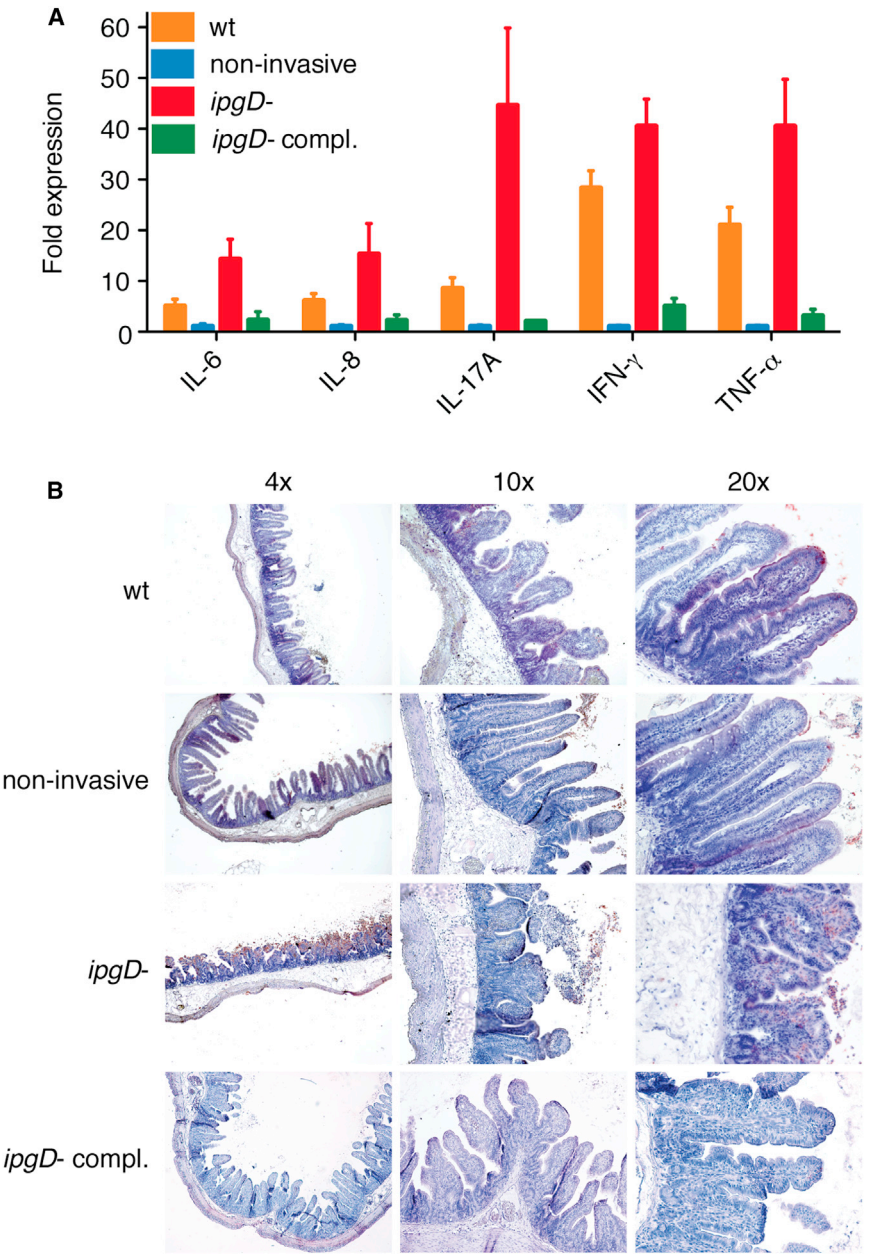

Figure 6. Inflammation Is Boosted upon Infection with *ipgD*-Deficient *Shigella*

Ligated ileal loops of rabbits were infected with *Shigella* for 7 hr.

(A) Quantitative real-time PCR analysis for selected cytokines. Folds of expression are given with respect to samples infected with the noninvasive strain (equal to 1). The mean of duplicate loops with range of expression is shown.

(B) Histological analysis. *Shigella*-LPS was immunohistochemically labeled (red), and sections were counterstained with hematoxylin. The data are from one representative rabbit of four. See also Figure S6 and Table S5.

fashion by epithelial and mucosal immune cells. Concomitantly, IpgD is injected, eventually forcing hemichannel closure and stopping ATP release. IpgD has the characteristic necessary to rapidly suppress ATP release: it is secreted in high amounts at the very beginning of infection (Niebuhr et al., 2000) and hydrolyses an abundant substrate—PtdIns(4,5)P_2—yielding a normally scarce product—PtdIns5P (Coronas et al., 2007; Keune et al., 2011; Sarkes and Rameh, 2010)—such that small changes in its abundance can be extremely efficient. Fast action is necessary because ATP release is nearly instantaneous, quicker than a transcriptional shift toward a proinflammatory cytokine profile. Moreover, owing to signal amplification and wide spectrum of target cells, eATP is a very potent mediator (Bours et al., 2006; Mariathasan et al., 2006). Altogether, these attributes might explain the striking difference we observed between tissues infected with WT or *ipgD*-deficient *Shigella*.

The results obtained with *Salmonella* and EPEC further indicate that regulated ATP release is a common intestinal epithelial response to infection with enteric pathogens. However, the finding that LPS (De Vuyst et al., 2007) and peptidoglycan (Robertson et al., 2010) can trigger hemichannel opening in epithelial cells in vitro indicates that the significance of regulated ATP release to infectious diseases might be much broader. How other pathogens such as *Salmonella* and EPEC avoid the potentially inflammatory effect of eATP remains to be elucidated. The T3SS effector SopB from *Salmonella* shares a conserved phosphatase motif with IpgD (Ungewickell et al., 2005), but its product-specificity is different (Marcus et al., 2001; Norris et al., 1998; Zhou et al., 2001). SopB likely only produces very little PtdIns5P compared to IpgD, which mediates hemichannel closure. Accordingly, SopB does not block hemichannel-dependent ATP release. The T3SS effector BopB from *Burholderia pseudomallei* shares the same phosphatase motif (Ungewickell et al., 2005), but the output of its enzymatic activity is not characterized.

The concept of endogenous danger signal has emerged to explain sterile inflammation and autoimmune diseases, as opposed to detection of non-self molecules during infection (Bours et al., 2006). Indeed, it is generally thought that activation of pattern-recognition receptors, which bind structures of microbial origin, initiates the inflammatory reaction against invading pathogens (Kawai and Akira, 2011). Therefore, the contribution of endogenous danger signals to the response against infection has not been fully appreciated so far. Particularly, infection-induced eATP accumulation has been documented in vitro in either epithelial cells or macrophages for few pathogens only, including *Shigella* (Tran Van Nhieu et al.,

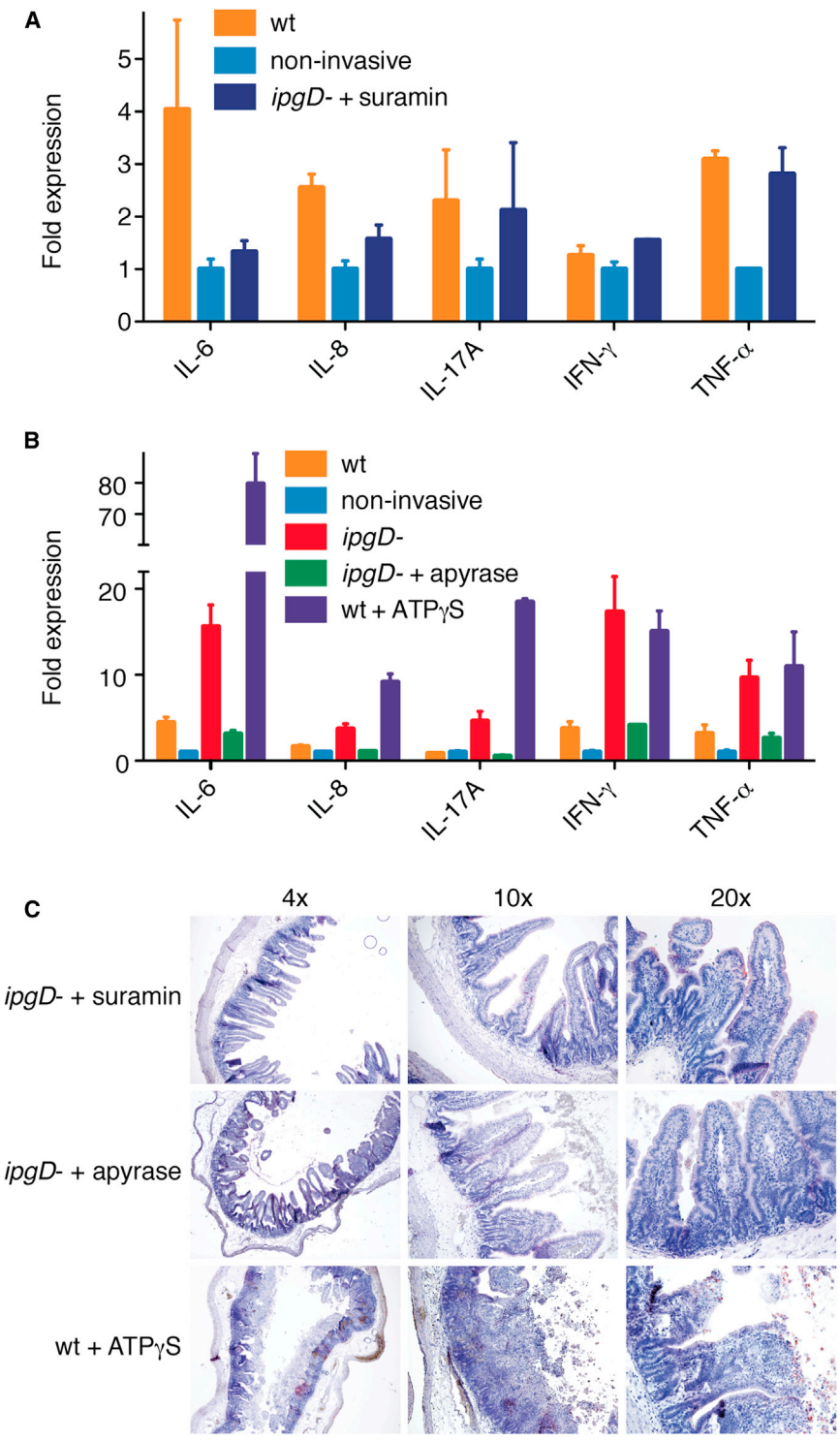

Figure 7. Inflammation Is Boosted by eATP upon Infection with *Shigella*

Ligated ileal loops of rabbits were infected with *Shigella* for 7 hr.

(A) Quantitative real-time PCR analysis for selected cytokines of samples infected in the presence or absence of 50 μM suramin. The mean of duplicate loops with range of expression is shown.

(B) Quantitative real-time PCR analysis for selected cytokines of samples infected in the presence or absence of 750 U apyrase or 400 μM ATPγS. The mean of duplicate loops with range of expression is shown.

(C) Histological preparations of samples A-B. *Shigella*-LPS was immunohistochemically labeled (red) and sections were counterstained with hematoxylin. The data are from representative rabbits of four to six per condition. See also Figure S6 and Tables S6 and S7.

2003), uropathogenic *Escherichia coli* (Säve and Persson, 2010), *Bacillus anthracis* (Ali et al., 2011), *Treponema denticola* (Jun et al., 2012), *Chlamydia trachomatis* (Pettengill et al., 2012), and HIV-1 (Séror et al., 2011).

Several other potentially anti-inflammatory factors have been described in *Shigella* and other pathogenic bacteria. They mostly prevent NF-κB activation, the master regulator of proinflammatory cytokines, by altering well-described pathways such as ubiquitin-dependent protein degradation and MAPK signaling (Sansonetti and Di Santo, 2007). IpgD's unique mode of action allowed us to identify PtdIns5P as key component of hemichannel regulation. Both synthesis and functions of PtdIns5P (Coronas et al., 2007; Keune et al., 2011) and regulation of hemichannels are poorly studied (Evans et al., 2006). How PtdIns5P restrains hemichannel function is currently under investigation.

The intestinal mucosa is a unique site of contact with microorganisms, where fine-tuned mechanisms permit tolerance of commensals and immunity to pathogens. Rupture of this balance has catastrophic consequences on human health (Sansonetti, 2011). Thus, understanding how the immune system discriminates pathogens from commensals to juggle immune tolerance of microbiota and eradication of pathogens is of outstanding importance. Low levels of microbiota-derived eATP induce basal levels of intestinal Th17 cells (Atarashi et al., 2008), contributing to the maintenance of physiologic inflammation. The present study shows that regulated release of high levels of ATP induce tissue-destructive inflammation during *Shigella* infection. Probably, exaggerated ATP release is a fundamental mechanism enticing rupture of mucosal homeostasis and hence relevant to other enteric pathologies—both infectious and not—and to other tissues.

Our data provide new strategies for the development of drugs. Indeed, although eATP is a well-established proinflammatory signal, to date only agents targeting purinergic receptors are available for therapy, but none regulating ATP release (Dinarello, 2010; North and Jarvis, 2013). Chronic inflammatory diseases such as cancer, atherosclerosis, obesity, type 2 diabetes, allergies, and neurodegenerative and demyelinating disorders are major killers with steadily rising incidence, for some of which the contribution of eATP has been documented. To which extent hemichannel-dependent ATP release participates in these pathologies, and which Cx types are involved, remains to be clarified, but our work shows the great potential of candidate drugs targeting the hemichannel-eATP axis.

EXPERIMENTAL PROCEDURES

Cell Culture

Because HeLa cells lack Cx expression (Elfgang et al., 1995), stable Cx-transfectants were used. HeLa cells expressing Cx26 or Cx43 (Paemeleire et al., 2000) were kept in DMEM supplemented with 100 U/ml penicillin, 100 μg/ml streptomycin, and 10% heat-inactivated FBS at 37°C and 10% CO_2 in a humid environment. For TC7 cells, the medium was further supplemented with nonessential amino acids (100× stock solution). For infections, cell were kept in medium devoid of antibiotics for at least 24 hr. Cells were tested for mycoplasma on a regular basis with the MycoAlert mycoplasma detection kit (Lonza). Except for plaque formation assays, polarized TC7 cells were obtained with the Biocoat Intestinal Epithelium Differentiation Environment in the 24-well format (BD Biosciences) according to the manufacturer's instructions. For plaque formation assays, 10^6 cells per well were seeded in 6-well plates and allowed to differentiate for 21 days with two weekly changes of medium.

Bacterial Strains and Infections

WT *Shigella flexneri* serotype 5a strain M90T (Allaoui et al., 1992), the non-invasive *mxiD* mutant (Allaoui et al., 1993b), the *ipgD* mutant SF701, and the complemented *ipgD* mutant SF709 (Allaoui et al., 1993a) were described previously. WT *Salmonella enterica* serovar Typhimurium strain SL1344 and the *sopB*-deficient mutant (Humphreys et al., 2009) were a kind gift from Vassilis Koronakis and Daniel Humphreys (University of Cambridge, UK), and WT enteropathogenic *Escherichia coli* (EPEC) serotype O127:H6 strain E2348/69 from Jean-Philippe Nougayrède (INRA/ENV, Toulouse, France). Bacterial strains were conserved as glycerol stocks at −80°C.

Shigella was streaked out on soybean-casein digest agar containing 0.01% (w/v) Congo red and grown overnight at 37°C to select virulent colonies. For in vitro infections, a single colony was picked, grown overnight at 37°C and 200 rpm in soybean-casein digest broth, with antibiotics if indicated, and a 200-fold dilution subcultured to OD_{600nm} = 0.3–0.5. Bacteria were diluted in DMEM devoid of phenol red or HBSS supplemented with 20 mM HEPES/NaOH pH 7.4 to the desired MOI. *Shigella* expressing the adhesin AfaE (Clerc and Sansonetti, 1987) was used, except for plaque formation and gentamicin-protection assays. For infections with AfaE-bearing *Shigella*, cells were carefully rinsed twice with solution at room temperature, and bacteria were allowed to adhere to cells for 15 min, then the supernatant was discarded and replaced with warm solution for incubations at 37°C and 5% CO_2 for the indicated time. For in vivo infections, 300 μl of a 7 hr liquid culture were spread on soybean-casein digest agar and grown overnight at 37°C. Bacteria were suspended in 0.9% NaCl solution at the desired dose shortly before infections.

Salmonella and EPEC were streaked out on Luria-Bertani (LB)-agar to isolate colonies. For infections a single colony was picked, grown overnight at 37°C and 200 rpm in LB-broth, with antibiotics if indicated, and diluted in DMEM devoid of phenol red to the desired MOI.

Induction of Hemichannel Opening

Hemichannel opening was either induced by depletion of extracellular Ca^{2+} or by infection with *Shigella*. In the first case, cells were carefully rinsed twice with warm buffer (HBSS supplemented with 20 mM HEPES/NaOH pH 7.4) and once with buffer devoid of Ca^{2+} (further supplemented with 0.1 mM EGTA) or with Ca^{2+}-containing buffer for negative controls. Cells were then incubated for the indicated time points at 37°C either in buffer containing or devoid of Ca^{2+} to modulate hemichannel opening. For infections, AfaE-expressing *Shigella* was used as described above.

Quantification of ATP In Vitro

HeLa-Cx26 and nonpolarized TC7 cells were used at 80% confluency. Cells were treated in DMEM devoid of phenol red or HBSS supplemented with 20 mM HEPES/NaOH pH 7.4. Hemichannel opening was induced either by depletion of extracellular Ca^{2+} or by infection with *Shigella* at an MOI of 1:5 for HeLa-Cx26 cells and an MOI of 1:40 for polarized TC7 cells, as described above. Cells were incubated at room temperature with inhibitors for 15 min prior to stimulation. To determine the amount of eATP, we retrieved the supernatant quickly and filtered it by using Millex-GV Syringe-driven Filter Units with 0.22 μm pore size (Millipore) to remove detached cells or bacteria, if present. To determine the intracellular ATP content, we lysed cells for 10 min under rotation in ice-cold passive lysis buffer. ATP was quantified immediately with the firefly luciferase-based sensitive ATP Determination Kit (Biaffin) according to the manufacturer's instructions, as previously described (Tran et al., 2011a, 2011b). Briefly, samples were distributed in Lumitrac 200 white plates (Greiner Bio-One), mixed with an equal volume of assay solution and bioluminescence read in a MicroLumat *Plus* microplate LB96V Luminometer (EG&G Berthold) after 10 min of incubation. The background (from buffer) was subtracted and values of ATP concentrations of either noninfected or untreated cells were set to 1 for calculations and, if indicated, subtracted. Samples were prepared in triplicates or quadruplicates with separate cultures and precultures for infections.

For *Salmonella* and EPEC the procedure was similar, with the following modifications. For *Salmonella* HeLa-Cx26 and polarized TC7 cells were infected at an MOI of 1:2.5, but, because of the extremely quick interaction between host cells and the pathogen, the ATP assay solution was added directly to samples, just after bacterial suspensions. Luminescence was read in an Infinite M200 PRO multimode plate-reader (Tecan) at 37°C for 3–20 min of infection.

For EPEC polarized TC7 cells were infected at an MOI of 1:2.5. Bacteria were centrifuged onto cells at 180 × *g* for 10 min at room temperature, and then the supernatant was discarded and replaced with warm medium. Because of the slow interaction between host cells and the pathogen, preheated BSA-treated activated charcoal (10 mg) was added to samples to protect eATP, and infections were allowed to proceed for 2 hr at 37°C and 5% CO_2. Charcoal was carefully retrieved and processed as for in vivo eATP determinations.

Dye Uptake

Because the extent of cellular dye uptake is proportional to dye concentration, exposure time, temperature and, importantly, to the number of active hemichannels on the cell surface, dye uptake assays are routinely used to assess hemichannel opening. The uptake of the plasma membrane-impermeable, hemichannel-permeant fluorescent dye ethidium bromide was quantified. HeLa-Cx26 and -Cx43 cells were seeded onto acid-washed glass coverslips. The following day, cells were transfected with plasmid pKNE16 encoding EGFP-tagged *ipgD*, pKNE17 encoding phosphatase-dead EGFP-tagged *ipgD* owing to a single-point mutation at the catalytic site (Cys438Ser) (Niebuhr et al., 2002), pcDNA3-GFP-Lyn-*INP54* encoding GFP- and Lyn-tagged Inp54p from *Saccharomyces cerevisiae* (Raucher et al., 2000), and pEGFP-N1 encoding EGFP for controls (Clontech). Transfections were performed with Effectene (QIAGEN) according to the manufacturer's instructions. Cells were used at 70% confluency 36 hr after transfection. Hemichannel opening was induced by depletion of extracellular Ca^{2+} as described above. If appropriate, 15 min prior to stimulation and during dye loading cells were treated with 100 μM 18α-glycyrrhetinic acid (AGA) in DMSO or with antibodies directed against the extracellular loop of Cx26 and Cx43—CELAb1 and CELAb2 (Clair et al., 2008)—that had previously been dialysed against (Ca^{2+}-free) PBS and were diluted 1:100 (v/v) in buffer. A buffer stock containing ethidium bromide was prepared to make sure that all samples were exposed to exactly the same concentration of dye. Cells were loaded with 5 μM ethidium bromide in buffer (containing Ca^{2+} for the negative control and devoid of Ca^{2+} for all other samples) for 10 min at 37°C as described in (Retamal et al., 2007). Then the supernatant was discarded and cells washed with buffer containing

Ca^{2+} to trap the dye in the cytosol. Images of at least ten random fields from three separate slides per condition were acquired within 30 min (the ethidium bromide signal was stable during this period) at 40× magnification using a DMRB_E fluorescence microscope (Leica Microsystems) equipped with a Cascade 512B CCD camera (Roper Scientific). Single transfected cells and their shape were distinguished thanks to GFP-fluorescence and intracellular ethidium bromide-fluorescence was quantified with the software MetaMorph (Molecular Devices). The background fluorescence was subtracted for every field. The mean ethidium bromide fluorescence of the positive control was set to 100 for calculations.

Infection of Rabbit Ileal Loops

The protocol was modified from Arondel et al., 1999 and approved by the Ethic Committee Paris 1 (number 20070004, December 9, 2007). Male New Zealand white rabbits weighing 2.5–3.0 kg (Charles River) were subjected to fasting the day before the experiment, and treatment of drinking water with 2.8 g l^{-1} sulfadimethoxine sodium salt (Mucoxid) to prevent coccidiosis was suspended. Rabbits were sedated with 0.25 mg kg^{-1} acepromazine maleate and anesthetized with 20 mg kg^{-1} ketamine. Before laparotomy, 400 mg lidocaine was applied for local anesthesia. The ileum was exteriorized and up to 12 segments of 5 cm devoid of Peyer's patches separated by spacers of equal length were ligatured starting from the ileocaecal junction, without damaging the mesenteric vasculature. Per loop, 5×10^9 bacteria in 500 μl or vehicle as control were injected. If indicated, reagents were mixed with bacterial suspensions immediately prior to injection, assuming that loops weighed 5 g to calculate concentrations. Samples were prepared in duplicates with randomized positions. After 4–8 hr, rabbits were euthanized with 120 mg kg^{-1} sodium pentobarbital, the luminal content of loops was collected, and tissue samples were retrieved for histology and rtPCR.

Quantification of eATP In Vivo

Because ATP is extremely unstable in the extracellular space, it was adsorbed to BSA-treated activated charcoal to protect it from degradation in the intestinal lumen. Activated charcoal has the property of adsorbing great quantities of small organic molecules such as ATP. Charcoal was freshly saturated with BSA to prevent adherence to the intestinal epithelium. Briefly, 50 mg ml^{-1} each of activated charcoal and BSA were suspended in 0.9% NaCl solution and incubated overnight at 37°C under rotation. Charcoal was recovered by centrifugation, washed with several changes of 0.9% NaCl solution to remove unbound BSA, and kept at 4°C until use.

To quantify ATP, rabbit ileal loops were infected with *Shigella* strains in the presence of 40 mg BSA-treated activated charcoal and, if indicated, hemichannel inhibitors as described above. Samples were prepared in duplicates. After 4 hr, rabbits were euthanized and a lavage of loops was performed with 0.5–2 ml ice-cold 0.9% NaCl solution. The luminal content was collected and immediately transferred to ice water. Charcoal was recovered by centrifugation at 16,000 × g and 4°C for 2 min and washed three times with ice-cold solution. To eliminate bacteria, we incubated samples with 50 μg ml^{-1} each of gentamicin and ceftriaxone for 45 min at 37°C under rotation, washed them, and kept them at 4°C until the next day. ATP was eluted from charcoal by three successive 30 min incubations with 10% (v/v) pyridine at 4°C under rotation. Eluates were pooled and dried in a SVC-100H Speed Vac concentrator (Savant) because the ATP assay could not be performed in the presence of pyridine. The pellet was dissolved in double-distilled water, and ATP was quantified immediately with the firefly luciferase-based sensitive ATP Determination Kit (Biaffin) as described above. The ATP content of individual samples was extrapolated from the background-subtracted standard curve, and the mean with SD of corresponding duplicate loops was obtained. To verify the integrity of the mucosa and to assess the progress of the inflammatory response, tissue samples were retrieved for analysis by histology and quantitative RT-PCR.

Quantification of eATP Breakdown Products In Vivo

To quantify ATP breakdown products, we infected rabbit ileal loops with various *Shigella* strains with or without hemichannel inhibitors as described above. Samples were prepared in duplicates. After 4 hr, rabbits were euthanized and a lavage of loops was performed with 0.5–2 ml ice-cold 0.9% NaCl solution. The luminal content was collected, immediately transferred to ice water, and weighed. Samples were spun at 16,000 × g and 4°C for 10 min to remove insoluble material, transferred to clean tubes, and kept at −80°C. Luminal fluids were defrozen on ice and diluted 1:10 in ice-cold buffer, and ATP breakdown products were measured using a fluorescence assay as described in (A.P. and P.J.S., unpublished data). The nucleoside and uric acid content of individual samples was extrapolated from the background-subtracted standard curve and the mean with SD of corresponding duplicate loops was obtained. To verify the integrity of the mucosa and to assess the progress of the inflammatory response, we retrieved tissue samples for analysis by histology and quantitative RT-PCR.

Histology

Samples were processed according to standard techniques for immunohistochemistry and hematoxylin counterstaining. Briefly, tissue was fixed for 2 days in 4% (w/v) paraformaldehyde in PBS, dehydrated with increasing concentrations of ethanol, and defatted with xylene according to standard protocols, embedded in paraffin, cut, and mounted on microscope slides (Superfrost Plus, Thermo Scientific). Samples were deparaffinized, rehydrated with increasing dilutions of ethanol, permeabilized with 0.1% (v/v) Triton X-100 in PBS, bleached with 3.3% hydrogen peroxide, and blocked with Ultra V Block solution (Lab Vision®). Bacteria were labeled with a monoclonal antibody directed against *S. flexneri* serotype 5a LPS (Phalipon et al., 1995) followed by a peroxidase-coupled secondary antibody (Envision+ System-HRP, Dako). Color was developed by addition of 3-amino-9-ethylcarbazole (AEC+ High Sensitivity Substrate-Chromogen, Dako). Sections were counterstained with hematoxylin and samples mounted with Aqua-Mount. Images were acquired on an Eclipse E800 microscope connected to a DXM1200F Digital Camera with the software ACT-1 (Nikon). For quantitative evaluation of samples, the length to width ratio of villi was scored with ImageJ (Abramoff et al., 2004).

Quantitative Real-Time PCR

Tissue samples of approximately 1g were retrieved from rabbit ileal loops and immediately homogenized in 5 ml TRIzol Reagent with an Ultra-Turrax T25 disperser (Janke & Kunkel, IKA Labortechnik, Staufen, Germany). Homogenates were centrifuged at 12,000 × *g* and 4°C for 10 min to remove insoluble material and stored at −80°C. RNA was extracted from a TRIzol-chloroform mixture (5:1 v/v) with MaXtract High Density Tubes (QIAGEN), precipitated by addition of isopropyl alcohol (1.2:1 v/v), and washed with 75% ethanol. To remove contaminating DNA, we dissolved RNA pellets in reaction buffer and digested them with RNase-free DNase I for 10 min at room temperature and purified them further with the RNeasy Mini Kit (QIAGEN). RNA concentration and purity were assessed with a NanoDrop 2000 Spectrophotometer (Thermo Scientific). RNA was kept at −80°C.

For cDNA synthesis, 2 μg of RNA were mixed with 0.5 μg of oligo$(dT)_{18}$ primer and heated to 70°C for 10 min. After addition of 200 U SuperScript II Reverse Transcriptase along with reaction buffer, 10 mM DTT, 0.5 μg each of dNTP, and 40 U RNasin Plus Ribonuclease Inhibitor, samples were incubated at 42°C for 1 hr. Enzymes were inactivated at 70°C for 5 min. cDNA was stored at −20°C.

For quantitative RT-PCR, 50-fold diluted cDNA was distributed in MicroAmp Optical 384-well Reaction Plates (Applied Biosystems) in duplicates and mixed with 0.2 μM each forward and reverse primer and Power SYBR Green PCR Master Mix (1:1 v/v). Primers were described in Schnupf and Sansonetti, 2012. Plates were sealed with MicroAmp Optical Adhesive Film (Applied Biosystems), and target sequences were amplified in a 7900HT Fast Real-Time PCR System (Applied Biosystems) under standard conditions: 2 min at 50°C and 10 min at 95°C, followed by 40 cycles composed of 15 s at 95°C and 1 min at 60°C. For quality control, a dissociation step was added at the end of the run. Data were analyzed with the Sequence Detection System v2.1 software (Applied Biosystems). Relative quantitation of gene expression with respect to samples infected with noninvasive *Shigella* was obtained using the comparative C_T method and the housekeeping gene glyceraldehyde 3-phosphate dehydrogenase (GAPDH) for input normalization.

Statistics

Statistical analysis was performed with the software Prism.

SUPPLEMENTAL INFORMATION

Supplemental Information includes six figures, seven tables, and Supplemental Experimental Procedures and can be found with this article online at http://dx.doi.org/10.1016/j.immuni.2013.11.013.

ACKNOWLEDGMENTS

We thank Huot Khun for suggestions concerning histology, Pamela Schnupf for sharing RT-PCR primers, and PMM members for critical reading. A.P. thanks Cesare Montecucco for introducing her to lipids. A.P. performed and analyzed all experiments, except PtdIns5P mass assays and in vivo infections, which were carried out with the help of H.T. and P.J.S., respectively. B.P. contributed tools and discussion. A.P., G.T.V.N., and P.J.S. designed research. A.P. wrote the manuscript. All authors corrected and approved the manuscript. A.P. was a recipient of subsequent EMBO Long-Term and Marie Curie Intra-European Fellowships. P.J.S. is an HHMI Investigator. This project was supported by ANR grant 2010 MIDI 007 01 to A.P. and P.J.S. and ERC Advanced Grant HOMEOEPITH to P.J.S.

Received: May 2, 2013
Accepted: October 9, 2013
Published: December 12, 2013

REFERENCES

Abramoff, M.D., Magelhaes, P.J., and Ram, S.J. (2004). Image Processing with ImageJ. Biophotonics International *11*, 36–42.

Ali, S.R., Timmer, A.M., Bilgrami, S., Park, E.J., Eckmann, L., Nizet, V., and Karin, M. (2011). Anthrax toxin induces macrophage death by p38 MAPK inhibition but leads to inflammasome activation via ATP leakage. Immunity *35*, 34–44.

Allaoui, A., Mounier, J., Prévost, M.C., Sansonetti, P.J., and Parsot, C. (1992). *icsB*: a *Shigella flexneri* virulence gene necessary for the lysis of protrusions during intercellular spread. Mol. Microbiol. *6*, 1605–1616.

Allaoui, A., Ménard, R., Sansonetti, P.J., and Parsot, C. (1993a). Characterization of the *Shigella flexneri ipgD* and *ipgF* genes, which are located in the proximal part of the *mxi* locus. Infect. Immun. *61*, 1707–1714.

Allaoui, A., Sansonetti, P.J., and Parsot, C. (1993b). MxiD, an outer membrane protein necessary for the secretion of the *Shigella flexneri* Ipa invasins. Mol. Microbiol. *7*, 59–68.

Arondel, J., Singer, M., Matsukawa, A., Zychlinsky, A., and Sansonetti, P.J. (1999). Increased interleukin-1 (IL-1) and imbalance between IL-1 and IL-1 receptor antagonist during acute inflammation in experimental Shigellosis. Infect. Immun. *67*, 6056–6066.

Atarashi, K., Nishimura, J., Shima, T., Umesaki, Y., Yamamoto, M., Onoue, M., Yagita, H., Ishii, N., Evans, R., Honda, K., and Takeda, K. (2008). ATP drives lamina propria T_H17 cell differentiation. Nature *455*, 808–812.

Bours, M.J., Swennen, E.L., Di Virgilio, F., Cronstein, B.N., and Dagnelie, P.C. (2006). Adenosine 5′-triphosphate and adenosine as endogenous signaling molecules in immunity and inflammation. Pharmacol. Ther. *112*, 358–404.

Clair, C., Combettes, L., Pierre, F., Sansonetti, P., and Tran Van Nhieu, G. (2008). Extracellular-loop peptide antibodies reveal a predominant hemichannel organization of connexins in polarized intestinal cells. Exp. Cell Res. *314*, 1250–1265.

Clerc, P., and Sansonetti, P.J. (1987). Entry of *Shigella flexneri* into HeLa cells: evidence for directed phagocytosis involving actin polymerization and myosin accumulation. Infect. Immun. *55*, 2681–2688.

Coronas, S., Ramel, D., Pendaries, C., Gaits-Iacovoni, F., Tronchère, H., and Payrastre, B. (2007). PtdIns5P: a little phosphoinositide with big functions? Biochem. Soc. Symp. *74*, 117–128.

De Vuyst, E., Decrock, E., De Bock, M., Yamasaki, H., Naus, C.C., Evans, W.H., and Leybaert, L. (2007). Connexin hemichannels and gap junction channels are differentially influenced by lipopolysaccharide and basic fibroblast growth factor. Mol. Biol. Cell *18*, 34–46.

Dinarello, C.A. (2010). Anti-inflammatory Agents: Present and Future. Cell *140*, 935–950.

Elfgang, C., Eckert, R., Lichtenberg-Fraté, H., Butterweck, A., Traub, O., Klein, R.A., Hülser, D.F., and Willecke, K. (1995). Specific permeability and selective formation of gap junction channels in connexin-transfected HeLa cells. J. Cell Biol. *129*, 805–817.

Evans, W.H., De Vuyst, E., and Leybaert, L. (2006). The gap junction cellular internet: connexin hemichannels enter the signalling limelight. Biochem. J. *397*, 1–14.

Humphreys, D., Hume, P.J., and Koronakis, V. (2009). The *Salmonella* effector SptP dephosphorylates host AAA+ ATPase VCP to promote development of its intracellular replicative niche. Cell Host Microbe *5*, 225–233.

Isfort, K., Ebert, F., Bornhorst, J., Sargin, S., Kardakaris, R., Pasparakis, M., Bähler, M., Schwerdtle, T., Schwab, A., and Hanley, P.J. (2011). Real-time imaging reveals that $P2Y_2$ and $P2Y_{12}$ receptor agonists are not chemoattractants and macrophage chemotaxis to complement C5a is phosphatidylinositol 3-kinase (PI3K)- and p38 mitogen-activated protein kinase (MAPK)-independent. J. Biol. Chem. *286*, 44776–44787.

Jun, H.K., Lee, S.H., Lee, H.R., and Choi, B.K. (2012). Integrin $\alpha5\beta1$ activates the NLRP3 inflammasome by direct interaction with a bacterial surface protein. Immunity *36*, 755–768.

Kawai, T., and Akira, S. (2011). Toll-like receptors and their crosstalk with other innate receptors in infection and immunity. Immunity *34*, 637–650.

Keune, Wj., Bultsma, Y., Sommer, L., Jones, D., and Divecha, N. (2011). Phosphoinositide signalling in the nucleus. Adv. Enzyme Regul. *51*, 91–99.

Konradt, C., Frigimelica, E., Nothelfer, K., Puhar, A., Salgado-Pabon, W., di Bartolo, V., Scott-Algara, D., Rodrigues, C.D., Sansonetti, P.J., and Phalipon, A. (2011). The *Shigella flexneri* type three secretion system effector IpgD inhibits T cell migration by manipulating host phosphoinositide metabolism. Cell Host Microbe *9*, 263–272.

Madara, J.L., Patapoff, T.W., Gillece-Castro, B., Colgan, S.P., Parkos, C.A., Delp, C., and Mrsny, R.J. (1993). 5′-adenosine monophosphate is the neutrophil-derived paracrine factor that elicits chloride secretion from T84 intestinal epithelial cell monolayers. J. Clin. Invest. *91*, 2320–2325.

Marcus, S.L., Wenk, M.R., Steele-Mortimer, O., and Finlay, B.B. (2001). A synaptojanin-homologous region of *Salmonella typhimurium* SigD is essential for inositol phosphatase activity and Akt activation. FEBS Lett. *494*, 201–207.

Mariathasan, S., Weiss, D.S., Newton, K., McBride, J., O'Rourke, K., Roose-Girma, M., Lee, W.P., Weinrauch, Y., Monack, D.M., and Dixit, V.M. (2006). Cryopyrin activates the inflammasome in response to toxins and ATP. Nature *440*, 228–232.

Niebuhr, K., Jouihri, N., Allaoui, A., Gounon, P., Sansonetti, P.J., and Parsot, C. (2000). IpgD, a protein secreted by the type III secretion machinery of *Shigella flexneri*, is chaperoned by IpgE and implicated in entry focus formation. Mol. Microbiol. *38*, 8–19.

Niebuhr, K., Giuriato, S., Pedron, T., Philpott, D.J., Gaits, F., Sable, J., Sheetz, M.P., Parsot, C., Sansonetti, P.J., and Payrastre, B. (2002). Conversion of $PtdIns(4,5)P_2$ into PtdIns(5)P by the *S.flexneri* effector IpgD reorganizes host cell morphology. EMBO J. *21*, 5069–5078.

Norris, F.A., Wilson, M.P., Wallis, T.S., Galyov, E.E., and Majerus, P.W. (1998). SopB, a protein required for virulence of *Salmonella dublin*, is an inositol phosphate phosphatase. Proc. Natl. Acad. Sci. USA *95*, 14057–14059.

North, R.A., and Jarvis, M.F. (2013). P2X receptors as drug targets. Mol. Pharmacol. *83*, 759–769.

Paemeleire, K., Martin, P.E., Coleman, S.L., Fogarty, K.E., Carrington, W.A., Leybaert, L., Tuft, R.A., Evans, W.H., and Sanderson, M.J. (2000). Intercellular calcium waves in HeLa cells expressing GFP-labeled connexin 43, 32, or 26. Mol. Biol. Cell *11*, 1815–1827.

Parsot, C. (2009). *Shigella* type III secretion effectors: how, where, when, for what purposes? Curr. Opin. Microbiol. *12*, 110–116.

Pendaries, C., Tronchère, H., Arbibe, L., Mounier, J., Gozani, O., Cantley, L., Fry, M.J., Gaits-Iacovoni, F., Sansonetti, P.J., and Payrastre, B. (2006). PtdIns5P activates the host cell PI3-kinase/Akt pathway during *Shigella flexneri* infection. EMBO J. *25*, 1024–1034.

Pettengill, M.A., Marques-da-Silva, C., Avila, M.L., d'Arc dos Santos Oliveira, S., Lam, V.W., Ollawa, I., Abdul Sater, A.A., Coutinho-Silva, R., Häcker, G., and Ojcius, D.M. (2012). Reversible inhibition of *Chlamydia trachomatis* infection in epithelial cells due to stimulation of $P2X_4$ receptors. Infect. Immun. *80*, 4232–4238.

Phalipon, A., and Sansonetti, P.J. (2007). *Shigella*'s ways of manipulating the host intestinal innate and adaptive immune system: a tool box for survival? Immunol. Cell Biol. *85*, 119–129.

Phalipon, A., Kaufmann, M., Michetti, P., Cavaillon, J.M., Huerre, M., Sansonetti, P., and Kraehenbuhl, J.P. (1995). Monoclonal immunoglobulin A antibody directed against serotype-specific epitope of *Shigella flexneri* lipopolysaccharide protects against murine experimental shigellosis. J. Exp. Med. *182*, 769–778.

Ramel, D., Lagarrigue, F., Pons, V., Mounier, J., Dupuis-Coronas, S., Chicanne, G., Sansonetti, P.J., Gaits-Iacovoni, F., Tronchère, H., and Payrastre, B. (2011). *Shigella flexneri* infection generates the lipid PI5P to alter endocytosis and prevent termination of EGFR signaling. Sci. Signal. *4*, ra61.

Raucher, D., Stauffer, T., Chen, W., Shen, K., Guo, S., York, J.D., Sheetz, M.P., and Meyer, T. (2000). Phosphatidylinositol 4,5-bisphosphate functions as a second messenger that regulates cytoskeleton-plasma membrane adhesion. Cell *100*, 221–228.

Retamal, M.A., Schalper, K.A., Shoji, K.F., Bennett, M.V., and Sáez, J.C. (2007). Opening of connexin 43 hemichannels is increased by lowering intracellular redox potential. Proc. Natl. Acad. Sci. USA *104*, 8322–8327.

Robertson, J., Lang, S., Lambert, P.A., and Martin, P.E. (2010). Peptidoglycan derived from *Staphylococcus epidermidis* induces Connexin43 hemichannel activity with consequences on the innate immune response in endothelial cells. Biochem. J. *432*, 133–143.

Romero, S., Grompone, G., Carayol, N., Mounier, J., Guadagnini, S., Prevost, M.C., Sansonetti, P.J., and Van Nhieu, G.T. (2011). ATP-mediated Erk1/2 activation stimulates bacterial capture by filopodia, which precedes *Shigella* invasion of epithelial cells. Cell Host Microbe *9*, 508–519.

Sansonetti, P.J. (2011). To be or not to be a pathogen: that is the mucosally relevant question. Mucosal Immunol. *4*, 8–14.

Sansonetti, P.J., and Di Santo, J.P. (2007). Debugging how bacteria manipulate the immune response. Immunity *26*, 149–161.

Sarkes, D., and Rameh, L.E. (2010). A novel HPLC-based approach makes possible the spatial characterization of cellular PtdIns5P and other phosphoinositides. Biochem. J. *428*, 375–384.

Säve, S., and Persson, K. (2010). Extracellular ATP and P2Y receptor activation induce a proinflammatory host response in the human urinary tract. Infect. Immun. *78*, 3609–3615.

Schnupf, P., and Sansonetti, P.J. (2012). Quantitative RT-PCR profiling of the Rabbit Immune Response: Assessment of Acute *Shigella flexneri* Infection. PLoS One *7* (6), e36446.

Sellge, G., Magalhaes, J.G., Konradt, C., Fritz, J.H., Salgado-Pabon, W., Eberl, G., Bandeira, A., Di Santo, J.P., Sansonetti, P.J., and Phalipon, A. (2010). Th_{17} cells are the dominant T cell subtype primed by *Shigella flexneri* mediating protective immunity. J. Immunol. *184*, 2076–2085.

Séror, C., Melki, M.T., Subra, F., Raza, S.Q., Bras, M., Saïdi, H., Nardacci, R., Voisin, L., Paoletti, A., Law, F., et al. (2011). Extracellular ATP acts on $P2Y_2$ purinergic receptors to facilitate HIV-1 infection. J. Exp. Med. *208*, 1823–1834.

Tran, S.L., Guillemet, E., Ngo-Camus, M., Clybouw, C., Puhar, A., Moris, A., Gohar, M., Lereclus, D., and Ramarao, N. (2011a). Haemolysin II is a *Bacillus cereus* virulence factor that induces apoptosis of macrophages. Cell. Microbiol. *13*, 92–108.

Tran, S.L., Puhar, A., Ngo-Camus, M., and Ramarao, N. (2011b). Trypan blue dye enters viable cells incubated with the pore-forming toxin HlyII of *Bacillus cereus*. PLoS ONE *6*, e22876.

Tran Van Nhieu, G., Clair, C., Bruzzone, R., Mesnil, M., Sansonetti, P., and Combettes, L. (2003). Connexin-dependent inter-cellular communication increases invasion and dissemination of *Shigella* in epithelial cells. Nat. Cell Biol. *5*, 720–726.

Ungewickell, A., Hugge, C., Kisseleva, M., Chang, S.C., Zou, J., Feng, Y., Galyov, E.E., Wilson, M., and Majerus, P.W. (2005). The identification and characterization of two phosphatidylinositol-4,5-bisphosphate 4-phosphatases. Proc. Natl. Acad. Sci. USA *102*, 18854–18859.

Zhou, D., Chen, L.M., Hernandez, L., Shears, S.B., and Galán, J.E. (2001). A *Salmonella* inositol polyphosphatase acts in conjunction with other bacterial effectors to promote host cell actin cytoskeleton rearrangements and bacterial internalization. Mol. Microbiol. *39*, 248–259.